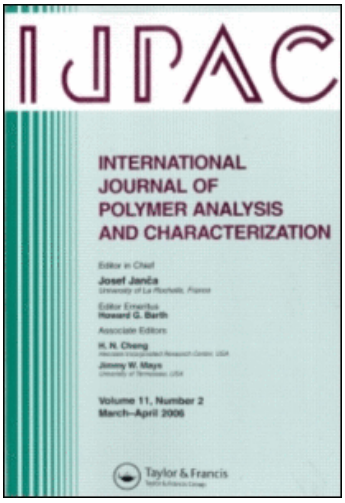

International Journal of Polymer Analysis and Characterization
Publication details, including instructions for authors and subscription information:
http://www.informaworld.com/smpp/title~content=t713646643

Polymer Analysis and Characterization by FTIR, FTIR-Microscopy, Raman Spectroscopy and Chemometrics

John M. Chalmers[a]; Neil J. Everall[a]
[a] ICI Technology, Wilton Research Centre, Wilton, Middlesbrough, Cleveland, UK

To cite this Article Chalmers, John M. and Everall, Neil J.(1999) 'Polymer Analysis and Characterization by FTIR, FTIR-Microscopy, Raman Spectroscopy and Chemometrics', International Journal of Polymer Analysis and Characterization, 5: 3, 223 — 245
To link to this Article: DOI: 10.1080/10236669908009739
URL: http://dx.doi.org/10.1080/10236669908009739

Int. J. Polym. Anal. Charact.,
1999 Vol. 5, pp. 223–245
Reprints available directly from the publisher
Photocopying permitted by license only

Polymer Analysis and Characterization by FTIR, FTIR-Microscopy, Raman Spectroscopy and Chemometrics*

JOHN M. CHALMERS† and NEIL J. EVERALL

ICI Technology, Wilton Research Centre, P.O. Box 90, Wilton, Middlesbrough, Cleveland TS90 8JE, UK

(Received 23 October 1998; In final form 22 January 1999)

FTIR-microspectroscopy and Raman spectroscopy, including FT-Raman spectroscopy, are now commonplace tools in many major industrial laboratories. When coupled with multivariate data analysis procedures, the spectroscopic data they produce can be utilized to provide not only rapid, cost-effective quality assurance methods for products, but also to enable simple, efficient or novel means to characterize physicochemical properties. In this paper we discuss these advantages and illustrate them through novel applications and case studies developed for the compositional analysis and physical structural characterization of polymeric products.

Keywords: FTIR; FTIR-microscopy; Raman; Chemometrics

INTRODUCTION

The vibrational spectroscopy techniques of mid-infrared and Raman are now commonly found in major industrial laboratories concerned with the analysis and characterization of polymeric materials and their products.[1,2] While Fourier transform infrared (FTIR) spectrometers are now almost singularly the choice for mid-IR use, both dispersive-Raman and FT-Raman instruments have their place. Both vibrational

* Presented at ISPAC-11 (International Symposium on Polymer Analysis and Characterisation), Santa Margerita, Italy, 25–27 May 1998.

†Corresponding author.

spectroscopy techniques are used extensively in combination with microscopes to provide spectral data at high spatial resolution,[1,3–5] although for Raman it is the dispersive systems that offer optimum performance in terms of spatial resolution and signal-to-noise ratio. Increasingly practised and of importance is the utilization of multivariate data analysis (*chemometric*) procedures. These, of which partial least squares (PLS) is probably presently the most frequently used for calibration purposes, offer many advantages and advances. They may be used for instance to provide the means to simple, robust quality assurance (QA) quantitative methods, to enhance the information content derived from vibrational spectra, or to facilitate process analysis routines.[2,6] Other chemometric algorithms allow for the classification of products according to spectral variations, which can hopefully be correlated with properties of interest.

In this paper we illustrate through three case studies the potential which recent developments and advances in vibrational spectroscopy practices offer to polymer analysis and chracterization. The first is concerned with process analysis, and considers the compositional analysis of a copolymer melt stream. The second involves determining by inference the morphology of a polymer. Finally, we probe both the molecular structure and physical characteristics of a polymer product with FTIR- and Raman-microscopies.

CASE STUDY 1: COMPOSITIONAL MONITORING OF PROPYLENE/ETHYLENE COPOLYMER MELT-STREAMS

Propylene/ethylene (P/E) copolymers are commercially important materials that have a wide range of physical and mechanical properties; these depend on not only the proportions of copolymerized propylene and ethylene, but also on their sequence lengths in copolymer chains. Mid-IR spectroscopic methods have been used for many years for determining off-line the composition of P/E copolymers, and as indicators of comonomer sequence distribution.[7,8] Most are based in some way on measurements of the absorbances associated with the methylene rocking mode vibrations of contiguous methylene units, which occur in the region 750–700 cm^{-1}. IR absorption bands at ~751, ~733, ~726 and ~722 cm^{-1} have been assigned to 2, 3, 4 and ≥ 5

contiguous methylene units respectively.[7] For the materials considered here, even number methylene sequences are of no consequence, since the production catalyst systems used did not invoke any head-to-tail insertion of propylene moieties into the copolymer chains. Notwithstanding, the analysis at room temperature over a wide compositional range is still complex. The IR absorption band for $(-CH_2-)_3$, arising from the sequence –PEP–, that is, an isolated ethylene unit, occurs near 733 cm^{-1}, which is overlapped by the absorption band for longer E sequences, which has a maximum near 720 cm^{-1}. Moreover, long E runs in a copolymer system can form crystalline domains and the rocking mode band is then replaced by a sharp and highly characteristic doublet with maxima near 720 and 730 cm^{-1}, the precise position and bandwidths of which are dependent somewhat on E sequence length and degree of crystallinity. This additional complication is removed, however, when the material is analyzed in the melt.[9–12] The absorption envelope attributable to copolymerized ethylene units may then be considered effectively as a three-component overlapped system, that is, a background from the low-wavenumber wing of the copolymerized propylene band near 810 cm^{-1}, an absorption band at 733 cm^{-1} due to copolymerized isolated E units, and an asymmetric band with a maximum near 720 cm^{-1} due to longer E sequences.

In addition, to circumventing complexities introduced by solid sample morphology, on-line analysis of a melt stream offers other advantages. Owing to the flow of material through the transmission melt cell during a measurement, significantly much more sample is examined in each measurement compared to a static, ambient temperature transmission measurement on a solid polymer film, in which only a few milligrams of material may be being interrogated. Another benefit lies in that a longer, fixed, and therefore reproducible, sample path-length is employed. In the study we report here, we have examined the feasibility and potential of utilizing a commercial process FTIR system for the compositional analysis of P/E copolymers in the range 0–10 wt% copolymerized E.

Experimental

The polymer melt-stream measurements were made on an IROS 100 (Automatik GmbH, Germany) IR process-control system.[13] It is

designed for continuous, rapid, monitoring of a polymer melt-stream by a FTIR spectrometer, which was an adapted Laser Precision Analytical (Analect) TRANSEPT III refractively scanned interferometer. It was operated over the mid-IR range (4000–400 cm^{-1}) using a DTGS detector. In our set-up, the system was connected to an extruder and the polymer melt flow fed into the IROS system by a gear pump. The polymer-melt at the process temperature passes through the special rheologically designed measuring melt channel cell, and then on to waste. The melt cell path-length for these measurements was set at 1 mm. It was fitted with 6-mm thick ZnSe windows. The extruder zone temperatures were set in the range 230–250°C; the speed control was set to deliver a flow of between 0.5 and 1 kg of material per hour. Polymer cell inlet, cell zones and outlet were set at temperatures between 240°C and 260°C.

Propylene homopolymer was used as the start-up material. When the system had reached the required temperatures and polypropylene was extruding at steady conditions, then spectroscopic measurements were commenced. Polypropylene was also used as the purge material.

The time for a single FTIR scan at 4 cm^{-1} spectral resolution was about 4 s. A single-beam reference (background) spectrum of 100 scans at 4 cm^{-1} resolution (2 × zero-filling) was recorded and up-dated at least once per day.

The sample evaluation procedure was:

(i) the feed hopper was emptied of unused sample,
(ii) the hopper was loaded with the next sample, and kept fed with sample during a measurement cycle,
(iii) the system was run (purged) with the sample for 15 min.
(iv) a melt spectrum of 500 scans at 4 cm^{-1} (2 × zero-filling) was recorded from each sample, waiting 2 min between the end of the scan set and the start of the next, if replicate measurements were to be made,
(v) return to (i).

The spectra were stored and saved on floppy discs for subsequent data processing, using GRAMS/32® (Galactic Industries Corp., Salem, USA).

The sample set of 40 samples was comprised of polypropylene and 17 samples that were copolymers in which the copolymerized ethylene

was mainly or totally present as isolated E units, which for convenience we will call random copolymers. The remainder of the samples were copolymers in which the ethylene was present as significantly longer runs, which we will from hereinafter refer to as block copolymers. The copolymerized ethylene contents of these samples had been pre-determined by local IR procedures developed by reference to NMR analyses for off-line laboratory-based analysis at ambient temperature of solid film specimens, for example, see Ref. [14,15]. These compositional values were used as the component concentration input to the PLS analysis.

Results and Discussion

Figure 1 shows the mid-IR absorbance spectrum recorded from a melt-stream of a polymer sample; while, Figure 2 shows the absorbance spectra over the range 780–650 cm^{-1} recorded from a range of samples. In the latter, the absorption maxima of the two copolymerized ethylene types are clearly evident. The isolated E units, that is $(-CH_2-)_3$, occur at 733.5 cm^{-1}, while longer sequences give rise to the feature near 719 cm^{-1}. Figure 3 shows the predicted versus actual copolymerized ethylene content mean-centered, four factor, cross-validated PLS correlation plot obtained from 106 IR absorbance spectra over the range 780–680 cm^{-1} recorded from 40 samples (13 in quadruplicate, 8 in triplicate, 11 in duplicate, and 8 as single scans).

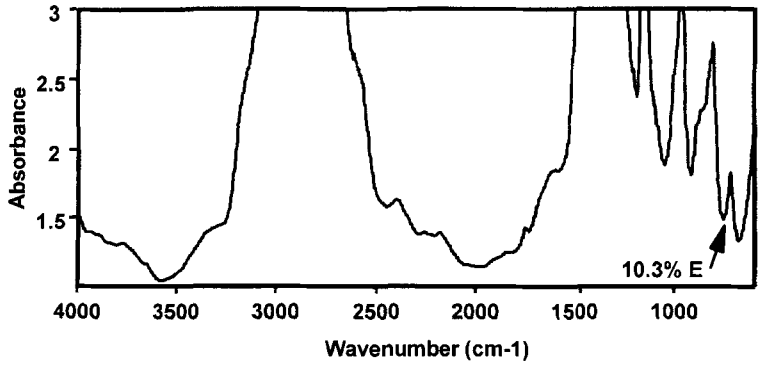

FIGURE 1 Mid-IR absorbance spectrum of a melt-stream of a P/E copolymer, containing 10.3% copolymerized ethylene.

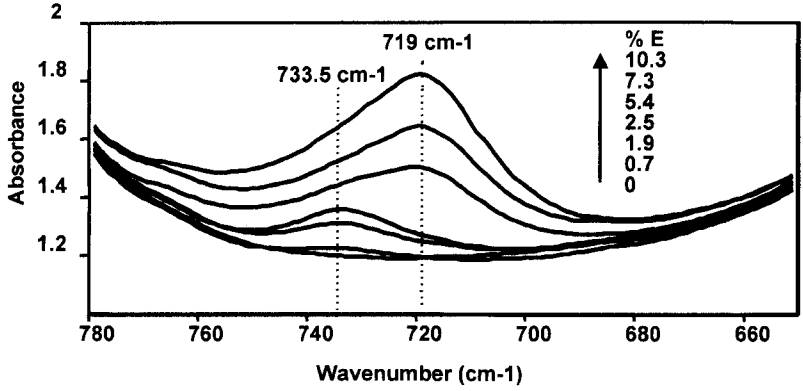

FIGURE 2 Melt-stream absorbance spectra recorded from a propylene homopolymer and a range of P/E copolymers. (E refers to ethylene.)

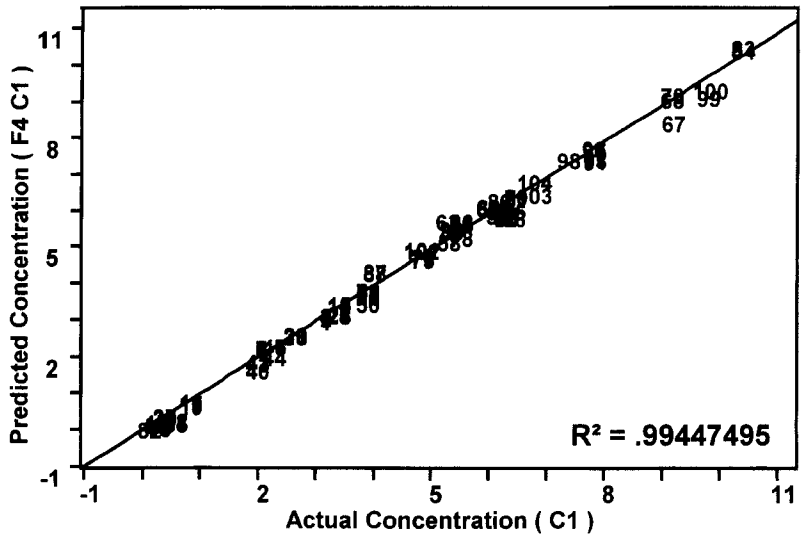

FIGURE 3 Predicted versus actual wt% concentrations mean-centered, four factor, cross-validated PLS correlation plot obtained from the set of P/E copolymer melt-stream absorbance spectra over the range 780–650 cm^{-1}.

Figure 4(a)–(c) show the PRESS, (Prediction Residual Error Sum of Squares), concentration residual and factors 3 and 4 loading plots associated with this PLS prediction plot, respectively. The PRESS plot indicated 4 factors as optimal for this experiment (F-test of 0.63), the

concentration residual plot shows a good spread of values and the PLS R^2 coefficient at 0.994 is high. (The correlation plots for factors 3 and 2 were not excessively different with R^2 values of 0.994 and 0.988, respectively, with associated F-test values of 0.76 and close to 1 respectively.)

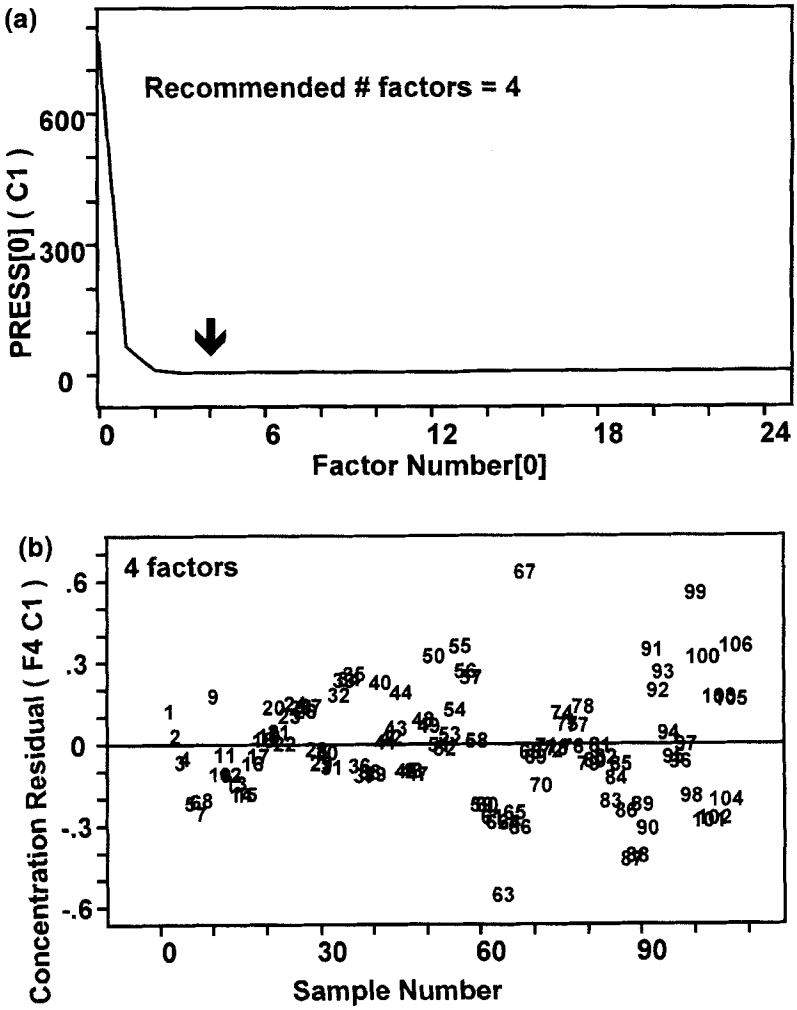

FIGURE 4(a) and (b)

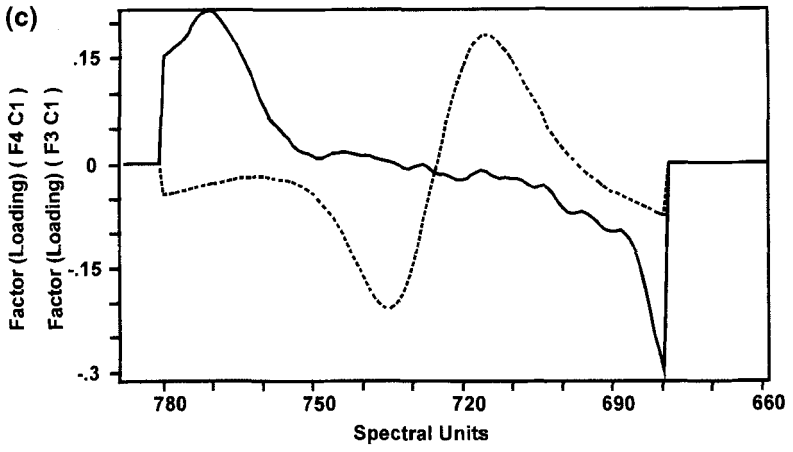

FIGURE 4(c)

FIGURE 4 (a) PRESS plot, (b) Factor 4 concentrations residuals plot and (c) Factor 4 (continuous line) and factor 3 (dashed line) loading plots associated with the PLS analysis shown in Figure 3.

Yet examination of the loadings plot shows that factor 4 is heavily influenced by the curvature of the background!

In order to further study the influences of the spectral data on the quantitative correlations, the data set was reduced to one from each sample, that is a sample set of 40, and then subjected to the GRAMS/32® PLS/IQ™ discriminant analysis algorithm. This is based on Mahalanoblis distance coupled with principal component analysis. Figure 5 shows the eigenvalue versus factor number plot output from this treatment, which is optimized at 8 factors. The scores plot from this analysis, shown in Figure 6, separates the set into essentially two groups. (Separations were observed similarly for factors 2–7 versus factor 1.) Those to the right of the abscissa value of 1 represent those copolymers which we have classified as random, while those to the left of this position are block copolymers. To emphasize the discrimination, we have in Figure 6 highlighted three spectra numbers from samples with very similar copolymerized ethylene contents, but which are readily separated according to their predominant sequence type, viz, samples 87 (3.9%), 71 (3.8%) and sample 24 (3.3%). Their spectra are shown in Figure 7.

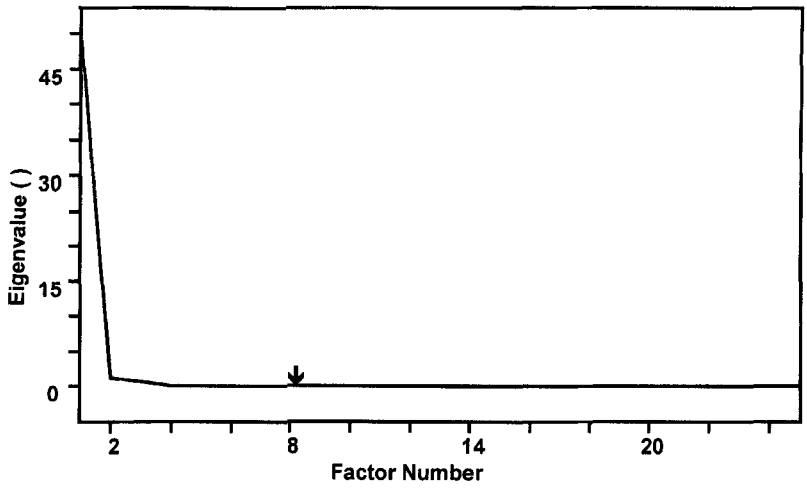

FIGURE 5 Eigenvalue versus, factor number plot output from discriminant analysis treatment of melt-stream P/E copolymer absorbance spectra data set over the range 780–650 cm^{-1}.

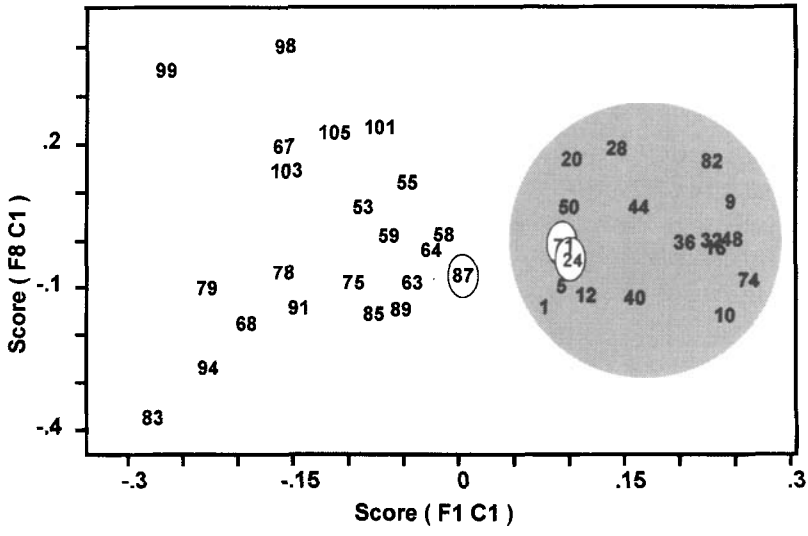

FIGURE 6 Scores plot from discriminant analysis treatment of melt-stream P/E copolymer absorbance spectra data set over the range 780–650 cm^{-1}. The shaded area contains all those copolymers designated as 'random'. The spectra of the three sample numbers highlighted, numbers 24, 71 and 87 are plotted in Figure 7.

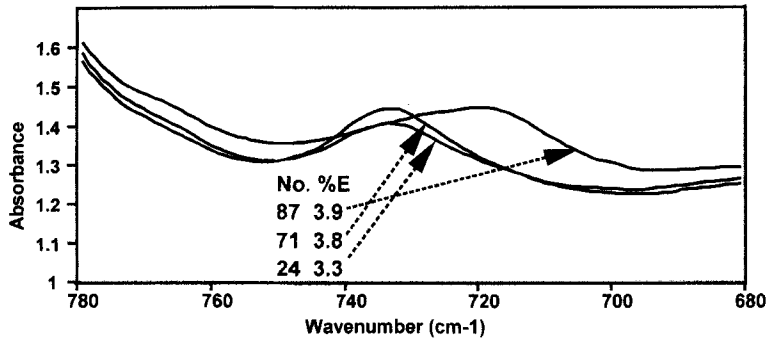

FIGURE 7 Melt-stream absorbance spectra numbers 24, 71 and 87 recorded from the three copolymer samples highlighted in Figure 6. (*E* refers to ethylene.)

TABLE I The data set used for the discriminant analysis treatment

Spectrum no.	*Ethylene* (wt%)	*Spectrum no.*	*Ethylene* (wt%)	*Spectrum no.*	*Ethylene* (wt%)
82*	0	87	3.9	67	9.1
10*	0.13	75	4.7	68	9.1
74*	0.17	103	4.7	99	9.7
48*	0.17	89	5.2	83	10.3
36*	0.28	63	5.2		
9*	0.4	58	5.2		
32*	0.46	64	5.4		
16*	0.73	78	5.4		
40*	1.9	59	5.9		
5*	2	53	6		
44*	2.2	85	6.1		
28*	2.6	105	6.2		
1*	3.1	55	6.2		
12*	3.3	79	6.4		
24*	3.3	101	6.6		
71*	3.8	98	7.3		
20*	3.8	94	7.7		
50*	3.8	91	7.7		

The asterisk indicates those copolymers which are designated as 'random'.

Table I lists the spectra set input to the discriminant analysis procedure; the first two columns are for the random copolymers, the remaining columns show data for the block copolymers. The loadings plot from this treatment shows a strong influence from the high-wavenumber tail of the absorbance band envelope. To minimize the effects of the background curvature and end of the input range discontinuities,

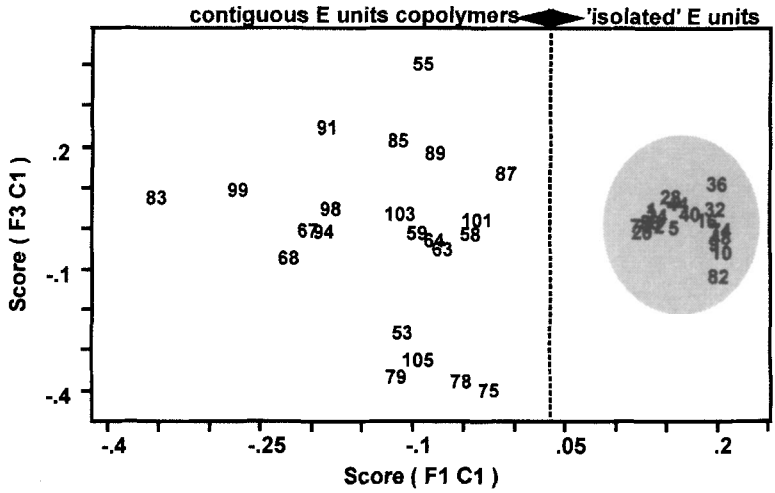

FIGURE 8 Factor 3 versus factor 1 scores plot obtained from the discriminant analysis treatment of the first-derivatives of the absorbance spectra over the range 780–680 cm^{-1} data set for the samples listed in Table I.

the data set input for discriminant analysis were pre-processed using a first-derivative algorithm. The subsequent eigenvalue versus factor plot now optimizes at a lower factor number, 5 (F-test value of 0.56). Figure 8 shows a scores plot from the first-derivative data set, in which the two types of copolymers now show much better discrimination along factor 1. Spectra numbers 53, 105, 79, 78 and 75 seem to form a block copolymer cluster which is extreme from spectrum number 55 along factor 3.

Examination of these spectra, see Figure 9, reveals those in the cluster to contain an additional absorbance feature near 665 cm^{-1}, which is most likely attributable to an additive. Further close examinations of other factor pair plots revealed other similar dependencies and influences outside of the absorbance envelope attributable to the copolymerized ethylene. Consequently, it was decided to reduce the spectral range being interrogated from 780–680 to 750–690 cm^{-1}. Figure 10 shows the factor 2 versus factor 1 discriminant analysis plot for the zero-order (non-first-derivative) set of 40 spectra over the range 750–690 cm^{-1}. Here, the data are again well separated along factor 1 according to type, while they seem to cluster further in respect of factor 2. The random-type copolymers align and separate essentially

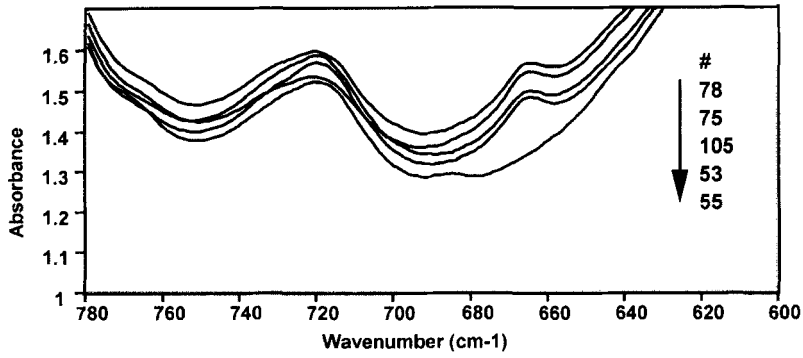

FIGURE 9 Melt-stream P/E copolymer absorbance spectra over the range 780–650 cm^{-1} recorded from sample numbers 53, 55, 75, 78 and 105.

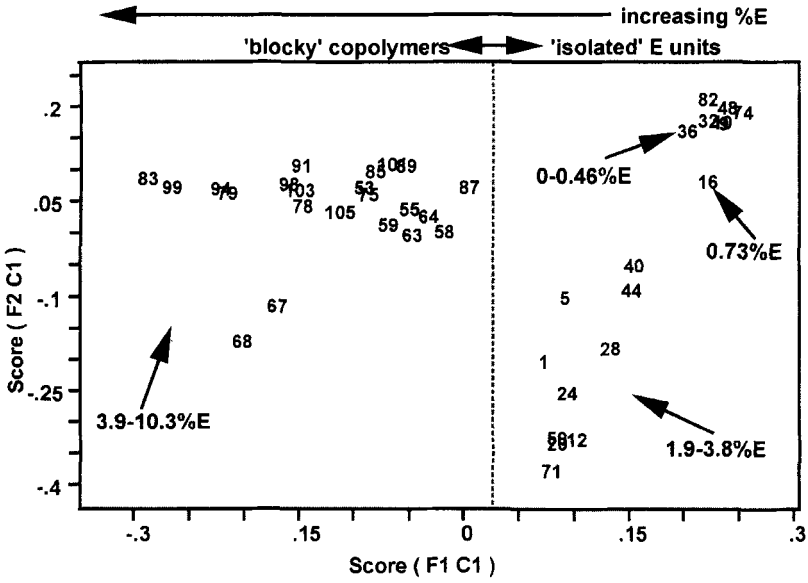

FIGURE 10 Factor 2 versus factor 1 scores plot obtained from the discriminant analysis treatment of the absorbance spectra over the range 750–690 cm^{-1} data set for the samples listed in Table I.

into two groups, according to ethylene content: those with copolymerized ethylene contents of less than 0.5%, and those with contents in the range 1.9–3.8%. The factor 2 loadings plot showed it be heavily influenced by the absorbances associated with copolymerized ethylene

types, minimizing near 733 cm^{-1}, while maximizing near 715 cm^{-1}. The full (nonderivatized) data set was then re-subjected to the PLS treatment, but this time with the input data limited to the spectral range 750–690 cm^{-1}. The PRESS plot now optimized at three factors (F-test of 0.5) and the predicted versus actual concentration plot had a similar R^2 coefficient of 0.995, see Figure 11, suggesting for this spectral data set a more robust calibration. This improved robustness is also mirrored in the SECV (standard error of cross-validation) or equivalent SEP (standard error of prediction) values for the two PLS models which were 0.200, for the 4-factor model using the spectral range 780–680 cm^{-1}, and 0.195 for the 3-factor model using the spectral range 750–690 cm^{-1}.

This analysis demonstrates clearly the feasibility for on-line compositional monitoring of P/E copolymer melt-streams by a process FTIR-spectroscopy system coupled with multivariate data analysis, certainly over the range 0.1–10 wt% copolymerized ethylene. In order to produce the more robust model, it was important to restrict the spectral range to screen out information that was noncorrelating with the desired property, and it was also key to effect removal of the curved baseline.

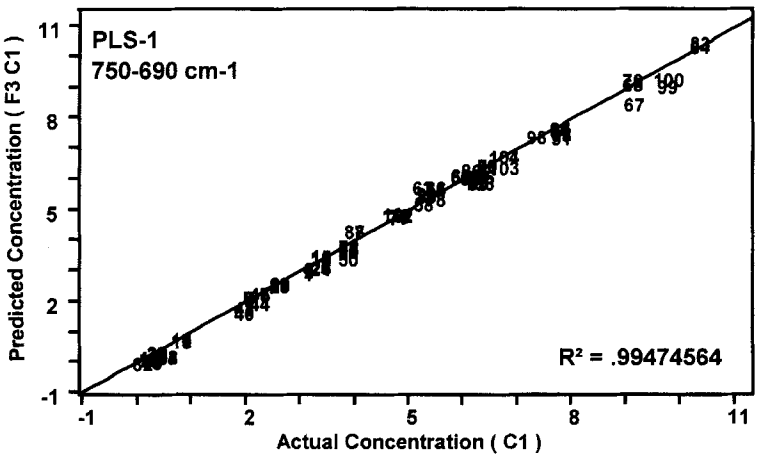

FIGURE 11 Predicted versus actual concentrations mean-centered, three factor, cross-validated PLS correlation plot obtained from the set of P/E copolymer melt-stream absorbance spectra over the range 750–690 cm^{-1}.

CASE STUDY 2: DENSITY AND ORIENTATION IN PET FILM AND CHIP SAMPLES BY FT-RAMAN SPECTROSCOPY

Inferring the morphology of a polymer, such as its crystallinity by measurement of its vibrational spectral characteristics is often, a more convenient, rapid and cost-effective means than more direct approaches.[2,16] Also, density can be an acceptable alternative to crystallinity for implying or monitoring the effects of process conditions on product properties.[2,16] FTIR,[17,18] Raman[17,19–22] and FT-Raman[16,23] measurements have all been used to provide measures of polymer crystallinity and density, including on-line Raman determinations.[24] Once developed the methods are readily extended to vibrational microspectroscopic mapping and profiling studies of physical property anisotropy and gradients. The work presented here to illustrate such an application is taken from a study on combined sample sets of poly(ethylene terephthalate) (PET) samples, comprising both a set of heat-crystallized PET chips and a set of heat-set uniaxial and biaxial drawn PET films of different draw ratios and differing densities.[16] The combined set covered the density ρ range 1.335–1.455 g cm^{-3}.

Experimental

The sample set comprised 15 heat-set chip samples with a spread of ρ from 1.3358 to 1.4073 g cm^{-3}, three heat-set uniaxially drawn films of draw ratios 2.5, 3.0 and 3.5 with densities of 1.3375, 1.3473 and 1.3491 g cm^{-3}, respectively, and seven heat-set 3.5×3.4 biaxially drawn film samples with a range of ρ of 1.3628–1.3998 g cm^{-3}. Full details of the sample set preparation and properties and experimental conditions may be found in Ref. [16]

The FT-Raman spectra were recorded on a Perkin-Elmer 1760 spectrometer (Perkin Elmer Ltd., Beaconsfield, UK), fitted with an InGaAs detector, which was operated at 77 K. Spectra comprised 40 scans each collected at 2 cm^{-1} resolution. A maximum laser power of 200 mW of the 1064 nm line of the Nd : YAG laser was used to avoid inducing crystallization. For the oriented-film samples, all spectra were recorded with the laser beam polarized parallel to the film's forward draw direction.

The FT-Raman data pre-processing and multivariate data analysis were performed using the Pirouette® software package (Infometrix Inc., USA). The spectral range 1800–600 cm^{-1} was used in the study, which was grouped at 8 cm^{-1} resolution, and all the spectra were normalized to constant area over the selected spectral region.

Results and Discussion

FT-Raman was used in preference to conventional dispersive-Raman with visible-laser excitation, since the spectra showed good, flat baselines; baseline correction was not needed, unlike the situation with visible-laser excitation where slight fluorescence baselines were observed.[21] Prior to multivariate data analysis, the spectra were all normalized to unit area to correct for differences in laser power, alignment, etc., and then mean-centered. Preliminary data analysis using HCA (hierarchical cluster analysis) and PCA (principal component analysis) showed that the lowest density amorphous chip was a distinct outlier and that the 1615 cm^{-1} band was exercising a strong influence on the derived principal components, which was not obviously directly related to density or orientation. The amorphous chip was the only sample which underwent no annealing. Consequently, the amorphous chip sample and the 1615 cm^{-1} region were both eliminated from further data analysis treatments. In a subsequent PCA analysis of this modified data set, PC1 primarily differentiated the samples on the basis of density, and the HCA dendogram showed more readily attributable clustering, see Figure 12. Figure 13 shows the cross-validated PLS 4-factor model for the modified PET sample set, for which the SEP is 0.0024 g cm^{-3}. The associated scores and loadings plots are shown in Figure 14. In the scores plot, factor 1 (PC1), which accounted for 47% of the variance, essentially distinguishes density, while, PC2, which accounted for 22% of the variance, separated samples primarily on the basis of orientation. The loadings plot reveals that an increase in ρ is correlated with a change in intensity of the C=O band near 1725 cm^{-1}; a narrowing of the C=O band is known to be associated with an increase in crystallinity.[16,25] It shows also that this is coupled primarily with changes in intensity of bands at 1094, 997 and 860 cm^{-1}; the bands at 1094 and 997 cm^{-1} are associated with the *trans* conformer of the PET glycol unit. Although separate cross-validated

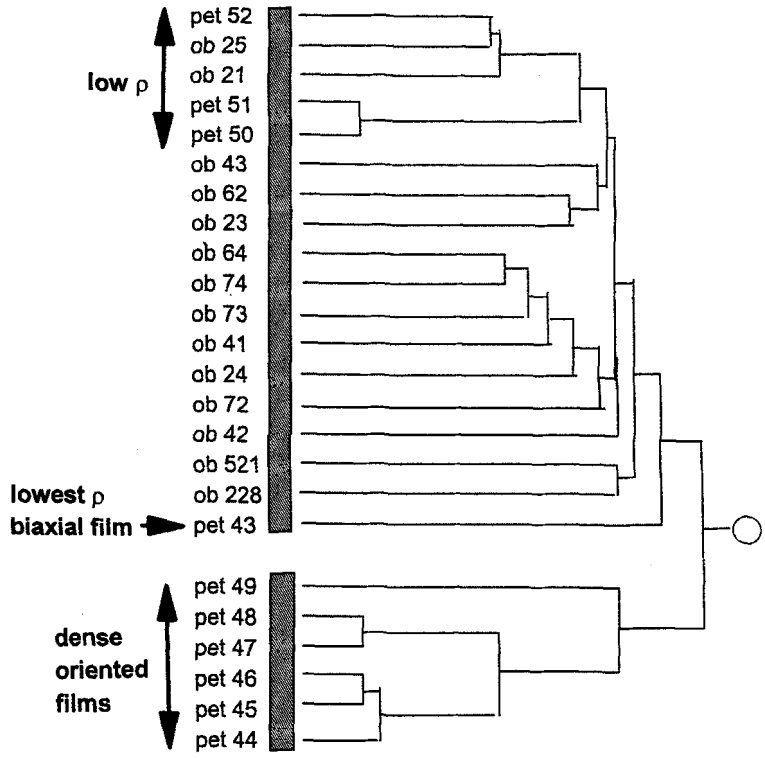

FIGURE 12 HCA dendogram from the FT-Raman spectra from the modified PET sample set, see text for details. Chip samples are coded 'ob'; film samples are coded 'pet'.

4-factor PLS models for the modified data set separated into chip and film samples gave SEPs of 0.0022 and 0.0023 $g\,cm^{-3}$ respectively, neither individual model was able to accurately predict the density of samples from the other sub-set.[16]

This study has demonstrated that PLS modeling can decouple the influences of crystallinity and orientation on Raman spectra, a nontrivial and perhaps impractical precision task using univariate techniques. The multivariate treatment is capable of providing a calibration for density for samples which spans both isotropic and anisotropic samples, yielding a model which was almost as precise as the individual models for the two sample types.

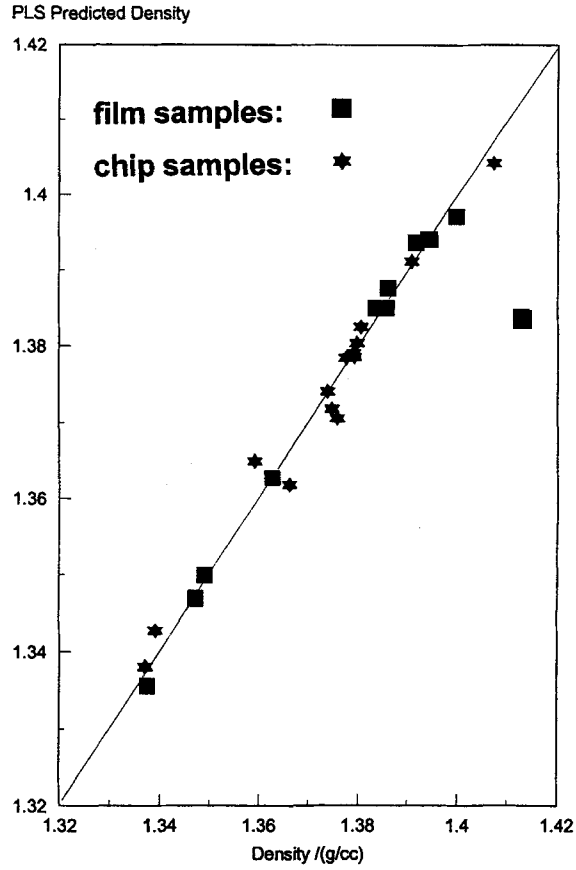

FIGURE 13 Cross-validated, 4-factor PLS model for the modified PET FT-Raman spectra data set.

CASE STUDY 3: END-GROUP AND DENSITY MAPPING THROUGH SOLID-STATE POLYMERIZED PET CHIP

In this case study, we use a combination of both FTIR-microscopy and Raman-microscopy to probe chemical structure and physical property differences through a polymer chip, and changes in these as a consequence of a solid-state polymerization process.[26] The characteristics measured were the end-group balance and density of products in the stages involved in the production of solid-state polymerized (SSP)

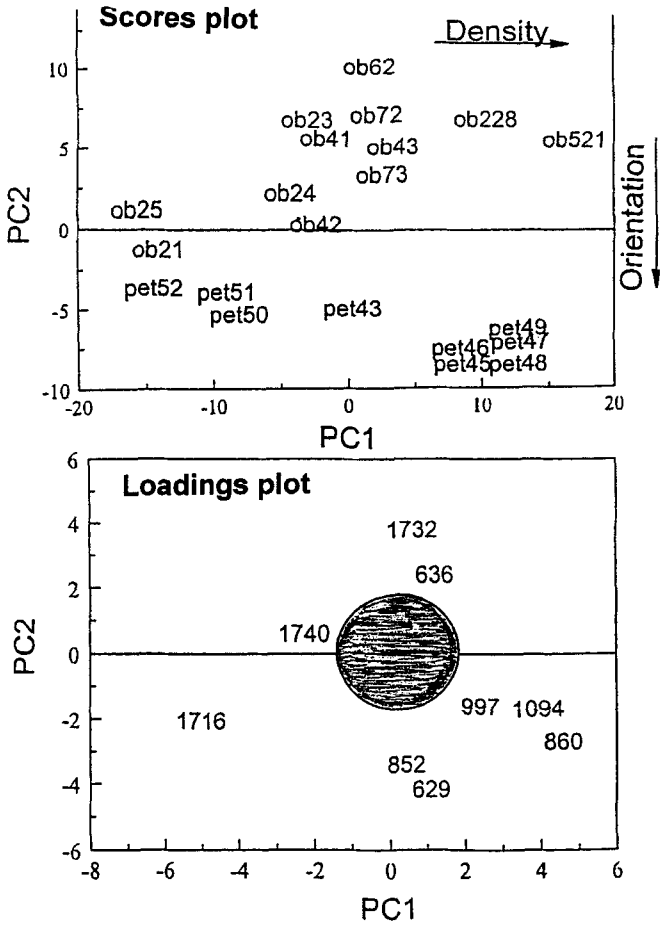

FIGURE 14 Factor 1 versus factor 2 scores and loadings plots associated with PLS analysis shown in Figure 13.

PET, a process designed to produce polymer that has a high intrinsic viscosity (IV) and is optimal for bottle manufacture and use. This process is shown schematically in Figure 15.

Experimental

The PET chip samples were oval in shape and approximately 2-mm long by 1.5-mm wide. The five-sample set comprised one each from

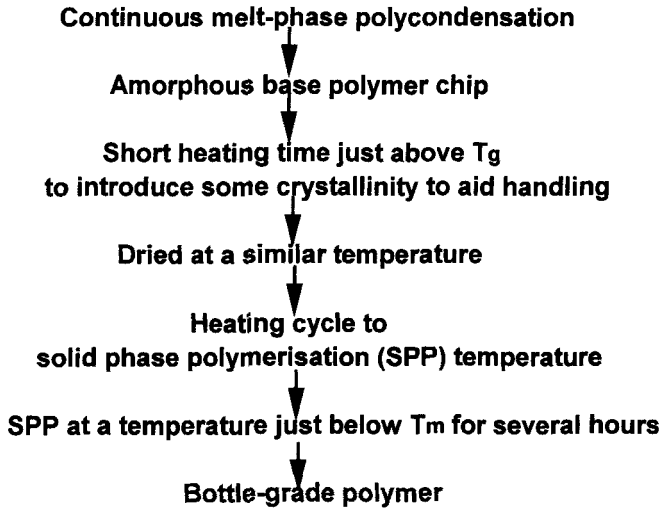

FIGURE 15 Schematic of the SPP PET process.

the key stages in the Solid-Phase Polymerization (SPP) process. Sections of nominal thickness 70-μm were microtomed from the center of the chip samples. Measurements of end-group concentration, –OH and –COOH, and sample density were then made at the chip section center and edge by FTIR-microscopy and Raman-microscopy, respectively. For the FTIR-microscopy, transmission measurements apertures of $20 \times 250\,\mu m$ were used to mask appropriate specimen areas. Care was taken to ensure that before the FTIR spectra were recorded that the sample under examination was dry, that is free from adsorbed water that would interfere with measurement of the –OH end group concentration. The alcoholic –OH was measured at $3542\,cm^{-1}$, while the carboxyl –OH was measured at $3256\,cm^{-1}$; their concentrations being determined using methods developed from those of Ward *et al.*,[27–29] which had been calibrated against NMR and chemical titration measurements, respectively. The FTIR-microscopy measurements were made on a Spectra-Tech IR-Plan FTIR-microscope (Spectra-Tech, Inc., Connecticut, USA) interfaced to a Mattson Cygnus FTIR spectrometer (Mattson Instruments, Inc., Madison, USA), at $4\,cm^{-1}$ resolution, 2000 scans per spectrum. The Raman-microscopy measurements were made using a Dilor XY Raman microscope (Instruments S.A., Longjumeau, France) with 514 nm excitation

and confocal pinhole. In these measurements the FWHM (full peak width at half maximum) of the C=O stretch was correlated with sample density (and hence crystallinity), based on the method of Melveger[25] but using in-house calibration.[16]

Results and Discussion

Figure 16 shows the FTIR spectra typical of those recorded from the center and close to the edge of a chip section, and the wavenumber positions at which the concentrations of the end-groups were determined. Figures 17 and 18 show plots typical of the changes observed in end-group concentrations at the center and near to the edge of a PET chip as a consequence of the SPP process. Overlaid on each figure is the associated change in material density as determined from Raman measurements.

The mapping measurements show:

(i) The –COOH and –OH end-group concentrations fall with the heat process applied in this SPP process.
(ii) There is an initial fall in the first heating stage.
(iii) The end-group concentrations then remain essentially constant through the drying and heating stage.
(iv) The solid-state polymerization stage causes further loss of both types of end-groups.

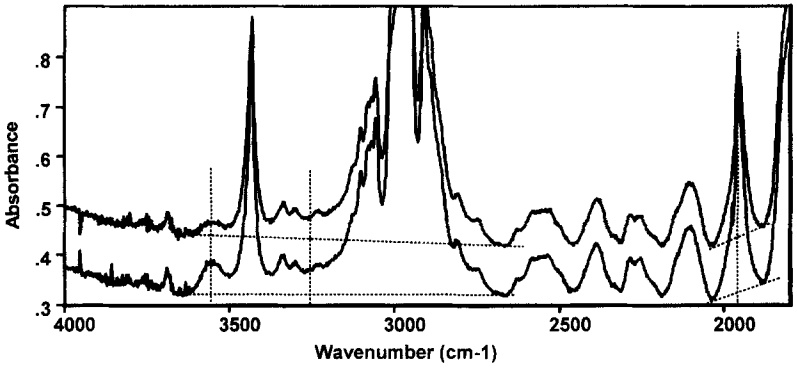

FIGURE 16 FTIR-microscopy absorbance spectra of PET chip sections: upper tracing, close to the edge; lower tracing, at the center. Dashed lines indicate positions at which peak maxima and baseline absorbance values were determined. The 1950 cm^{-1} band was used as an internal (thickness) reference band.

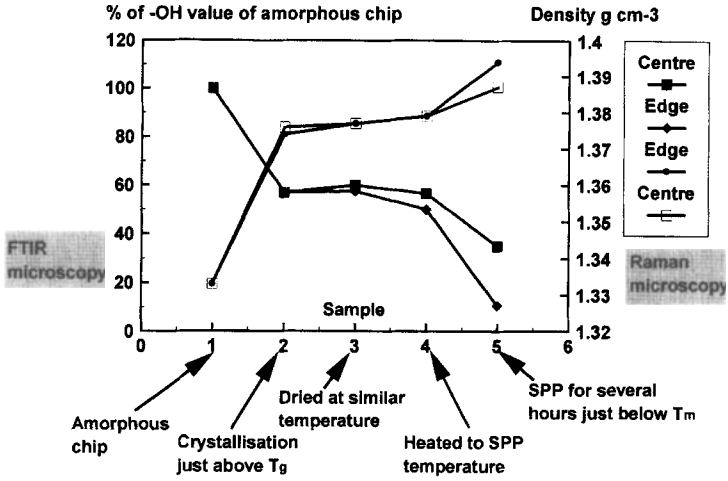

FIGURE 17 Comparison of –OH end-group concentrations, determined by FTIR-microscopy, and density, determined by Raman-microscopy, near the edge and at the center of a PET chip through the SPP process; ■ and ◆ refer to %OH, ● and □ refer to density.

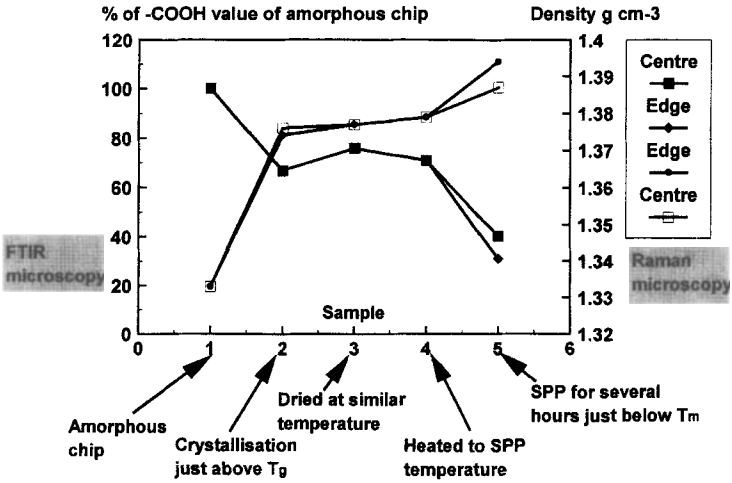

FIGURE 18 Comparsion of –COOH end-group concentrations, determined by FTIR-microscopy, and density, determined by Raman-microscopy, near the edge and at the center of a PET chip through the SPP process; ■ and ◆ refer to %COOH, ● and □ refer to density.

(v) For all chip samples except the SPP samples, there is no variation in end-group concentrations or in sample density across the chip.
(vi) For the SPP chip there is lower concentration of both –OH and –COOH end-groups near the chip edge as compared to the chip center.
(vii) There are concomitant increases in material density with decreases in end-group concentrations.

Through this study we have demonstrated clearly the value and potential of both FTIR-microscopy and Raman-microscopy to mapping or profiling chemical structure gradients and physical property anisotropy through polymer products.

CONCLUSION

We have through three case studies demonstrated modern approaches to the analysis and characterization of polymer products and processes within an industrial context. Multivariate data analysis procedures have been shown to be important and enhancing tools in both the process monitoring and product characterization applications. Vibrational spectroscopy–microscopy techniques have been shown to be invaluable to characterizing, mapping or profiling polymer product properties and structure at high spatial resolution.

Acknowledgments

Many colleagues at ICI were involved to differing extents in generating and analyzing the data of the three case studies presented here. In particular we would like to acknowledge Janet Lumsdon, who was primarily responsible for the end-group and crystallinity measurements on the PET chips, and Kay Atlay, who recorded most of the polymer melt-stream spectra. We would also like to thank ICI Technology for their permission to publish this paper.

References

[1] J.M. Chalmers and G. Dent (1997) *Industrial Analysis with Vibrational Spectroscopy* (The Royal Society of Chemistry, Cambridge, UK).

[2] J.M. Chalmers and N.J. Everall (1996) *TrAC*, **15**, 18.
[3] J.M. Chalmers and N.J. Everall (1995) *Macromol. Symp.*, **94**, 33.
[4] J.E. Katon (1994) *Vib. Spectrosc.*, **7**, 201.
[5] J.M. Chalmers, L. Croot, J.G. Eaves, N. Everall, W.F. Gaskin, J. Lumsdon and N. Moore (1990) *Spectrosc. Int. J.*, **8**, 13.
[6] D.C. Hassell and E.M. Bowman (1998) *Appl. Spectrosc.*, **52**, 18A.
[7] G. Bucci and T. Simonazzi (1964) *J. Polym. Sci.: C*, **7**, 203.
[8] A.H. Willbourn (1969) *Chem. Ind.*, 742, June 7.
[9] P.C. Ng, P.-L. Yeh, M. Gilbert and A.W. Birley (1984) *Polym. Commun.*, **25**, 250.
[10] P. Simak (1988) *Kunstoffe*, **78**, 234.
[11] J.M. Chalmers, A. Bunn, H.A. Willis, C. Thorne and R. Spragg (1988) *Mikrochim. Acta*, **I**, 287 (Recent Aspects of Fourier Transform Spectroscopy, Vol. 2 – *Proc. 6th Int. Conf. Four. Trans. Spec.*).
[12] H.A. Willis, J.M. Chalmers, A. Bunn, C. Thorne and R. Spragg (1988) *Analytical Applications of Spectroscopy*, C.S. Creaser and A.M.C. Davies, (Eds.) (Royal Society of Chemistry, London) pp. 188–200.
[13] The operating assets of the IROS product line of Automatik were purchased (June 1992) by FLOW VISION (Wilmington, USA), a subsidiary of the Kelvin Corporation. Subsequently, in June 1994, FLOW VISION was acquired by the Kayeness Division of Dynisco, Inc., USA.
[14] J.M. Chalmers (1976) *Proc. Int. IFAC Conf. Instrum. Autom. Pap., Rubber Plast. Ind.*, 3rd, 51.
[15] Method for low concentration ethylene copolymers based on a measure of the absorbance intensity at $\sim 733\,cm^{-1}$ (unpublished work).
[16] N. Everall, P. Tayler, J.M. Chalmers, D. MacKerron, R. Ferwerda and J.H. van der Maas (1994) *Polymer*, **35**, 3184.
[17] R.J. Lehnert, P.J. Hendra, N. Everall and N.J. Clayden (1997) *Polymer*, **38**, 1521.
[18] J.M. Chalmers, N.J. Everall and S. Ellison (1996) *Micron*, **27**, 315.
[19] R.J. Lehnert, P.J. Hendra and N. Everall (1995) *Polymer*, **36**, 2473.
[20] N. Everall, H. Owen and J. Slater (1995) *Appl. Spectrosc.*, **49**, 610.
[21] N. Everall, K. Davis, H. Owen, M.J. Pelletier and J. Slater (1996) *Appl. Spectrosc.*, **50**, 388.
[22] K.P.J. Williams and N.J. Everall (1995) *J. Raman Spectrosc.*, **26**, 427.
[23] N.J. Everall, J.M. Chalmers, R. Ferwerda, J.H. van der Maas and P.J. Hendra (1994) *J. Raman Spectrosc.*, **25**, 43.
[24] N.J. Everall (1995) In *An Introduction to Laser Spectroscopy*, D.L. Andrews and A.A. Demidov (Eds.) (Plenum Press, New York), pp. 115–131.
[25] A. Melveger (1972) *J. Polym. Sci. (A-2)*, **10**, 317.
[26] (a) J. Lumsdon, private communication; (b) J.M. Chalmers (1994) 1994 Pittsburgh Conference, Chicago, USA, February 27–March 4, paper 021, (c) J.M. Chalmers and N.J. Everall (1995) *Macromol. Symp.*, **94**, 33.
[27] D. Patterson and I.M. Ward (1957) *Trans. Faraday Soc.*, **53**(411), 291.
[28] I.M. Ward (1957) *Trans. Faraday Soc.*, **53**(419), 1406.
[29] I.M. Ward (1957) *Nature*, **180**, 141.